ELSEVIER

Neurobiology of Aging 31 (2010) 244–256

NEUROBIOLOGY OF AGING

www.elsevier.com/locate/neuaging

White matter pathology isolates the hippocampal formation in Alzheimer's disease

D.H. Salat [a,b,d,*], D.S. Tuch [a,b], A.J.W. van der Kouwe [a,b], D.N. Greve [a,b], V. Pappu [a,c], S.Y. Lee [a,c], N.D. Hevelone [a,c], A.K. Zaleta [a,c], J.H. Growdon [c], S. Corkin [a,d], B. Fischl [a,b], H.D. Rosas [a,c]

[a] *MGH/MIT/HMS Athinoula A. Martinos Center for Biomedical Imaging, Charlestown, MA, United States*
[b] *Department of Radiology, Massachusetts General Hospital, Boston, MA, United States*
[c] *Department of Neurology, Massachusetts General Hospital, Boston, MA, United States*
[d] *Department of Brain and Cognitive Sciences, Massachusetts Institute of Technology, Cambridge, MA, United States*

Received 17 October 2007; received in revised form 17 March 2008; accepted 22 March 2008
Available online 5 May 2008

Abstract

Prior work has demonstrated that the memory dysfunction of Alzheimer's disease (AD) is accompanied by marked cortical pathology in medial temporal lobe (MTL) gray matter. In contrast, changes in white matter (WM) of pathways associated with the MTL have rarely been studied. We used diffusion tensor imaging (DTI) to examine regional patterns of WM tissue changes in individuals with AD. Alterations of diffusion properties with AD were found in several regions including parahippocampal WM, and in regions with direct and secondary connections to the MTL. A portion of the changes measured, including effects in the parahippocampal WM, were independent of gray matter degeneration as measured by hippocampal volume. Examination of regional changes in unique diffusion parameters including anisotropy and axial and radial diffusivity demonstrated distinct zones of alterations, potentially stemming from differences in underlying pathology, with a potential myelin specific pathology in the parahippocampal WM. These results demonstrate that deterioration of neocortical connections to the hippocampal formation results in part from the degeneration of critical MTL and associated fiber pathways.

Keywords: Alzheimer; Aging; Diffusion tensor imaging; Fractional anisotropy; Diffusivity; MRI; White matter; Dementia; Hippocampus; Entorhinal; Memory; Axial diffusivity; Radial diffusivity; Tractography; Volume; Hyperintensities; T2; Myelin; Axon

1. Introduction

Careful histological examination of the brains of individuals with Alzheimer's disease (AD) has uncovered a probable substrate for the memory impairment in this condition. Specifically, layer-preferred degeneration in perirhinal and entorhinal cortices likely impedes the transfer of information from the neocortex to the hippocampus (Ball, 1978; Braak and Braak, 1991; Gomez-Isla et al., 1996; Hyman et al., 1984, 1986; Van Hoesen et al., 1991), thereby degrading the processing and storage of sensory input. Layer II of the entorhinal cortex shows profound alterations, including substantial loss of neurons even in the early stages of AD (Gomez-Isla et al., 1996). The projection termination zone of these fibers in the dentate gyrus of the hippocampal formation is also marked by degenerative changes, effectively resulting in a 'disconnection' between association and limbic cortices (Hyman et al., 1984, 1986). Given these important pathologic signatures, the majority of studies of mechanisms of AD symptomology have focused on medial temporal lobe (MTL) cortical degeneration. Nevertheless, these prior findings also implicate regional connectivity as a factor contributing to cognitive deterioration. Histological research demonstrates that brain white matter (WM) also degenerates in AD (Brun

* Corresponding author at: MGH/MIT/HMS Athinoula A. Martinos Center for Biomedical Imaging, MGH Department of Radiology, Building 149, 13th St., Mail Code 149 (2301), Charlestown, MA 02129-2060, United States. Tel.: +1 617 726 4704; fax: +1 617 726 7422.
E-mail address: salat@nmr.mgh.harvard.edu (D.H. Salat).

0197-4580/$ – see front matter © 2008 Elsevier Inc. All rights reserved.
doi:10.1016/j.neurobiolaging.2008.03.013

and Englund, 1986; Englund and Brun, 1990; Englund et al., 1988; Hyman et al., 1986). Brun and Englund (1986) reported a syndrome in 60% of AD patients of demyelination and axonal and oligodendroglial loss with accompanying gliosis in the deep WM that was independent from gray matter lesions. The authors suggested that the degeneration was potentially due to comorbid factors such as hypertension (Brun and Englund, 1986). WM disease, however, has been reported at autopsy in individuals with pure AD with no components of vascular brain disease (Sjobeck et al., 2006). Further, myelin staining is reduced in the perforant pathway, the main input fibers projecting neocortical information from the entorhinal cortex to the granule cells of the dentate gyrus in the hippocampal formation (Hyman et al., 1986). These findings suggest that at least some of the WM changes in AD are not due simply to comorbid factors, but are likely associated with AD pathological processes including MTL cortical pathology. The pathologic signatures spanning the perforant pathway, and the reduction in myelin integrity of this fascicle, underscores the potential influence of regional connectivity in the putative propagation of neurodegenerative events. An open question is whether such changes could be detected in patients *in vivo*, and whether this principal of degeneration in anatomically connected regions extends beyond the findings in the perforant pathway.

Neuroimaging studies have attempted to understand patterns and mechanisms of WM pathology in AD, and the clinical significance of such changes (de Leeuw et al., 2006), but the regional patterns and potential mechanisms of this WM pathology are still unclear. Moreover, whether WM changes are independent of classically described AD cortical pathology, such as hippocampal atrophy, is completely unknown. Total and regional WM volume is reduced in AD (Fotenos et al., 2005; Jernigan et al., 1991; Salat et al., 1999a,b, 2001; Stout et al., 1996), and WM signal abnormalities are associated with risk for cognitive decline (Au et al., 2006) and dementia (Prins et al., 2004), as well as an enhanced clinical syndrome in specific cognitive domains (Hirono et al., 2000). The use of WM signal abnormalities as a clinically relevant measure of WM pathology remains controversial because a number of studies report little consequence of this marker on clinical status (Mungas et al., 2005; Schmidt et al., 2002). Additionally, WM volume measures are limited because of the need to define regionally identifiable borders using morphometric landmarks, a particularly difficult task given the complex anatomy of WM and the limited information provided about this anatomy from a standard structural MR image.

Diffusion tensor imaging (DTI) has been applied extensively to understand the regional basis of tissue degeneration in a variety of clinical conditions including the study of normal aging (Moseley, 2002; Pfefferbaum et al., 2000, 2005; Pfefferbaum and Sullivan, 2003; Salat et al., 2005a,b; Sullivan et al., 2001, 2006; Sullivan and Pfefferbaum, 2006). Two primary metrics of the diffusion properties within a voxel, termed diffusivity and fractional anisotropy (FA) (Basser, 1995; Basser and Pierpaoli, 1996; Pierpaoli and Basser, 1996), have been commonly employed as indices of tissue pathology. More recently, studies by Song and colleagues utilizing animal models demonstrate that the diffusivity measure can be further subdivided in to axial and radial components, which could provide information on axonal and myelin pathology selectively (Budde et al., 2007; Song et al., 2002, 2003). Rose and colleagues (Rose et al., 2000) demonstrated altered diffusion measures in the splenium of the corpus callosum, the superior longitudinal fasciculus, cingulum, and internal capsule in patients with AD, and in parahippocampal, thalamic, and cingulate WM in individuals with mild cognitive impairment (Rose et al., 2006). Diffusion measures were related to indices of disease severity and cognitive ability and the specific association with episodic memory presents a potential clinical role for DTI to index WM degeneration and track AD symptoms. Other studies have found altered diffusion measures in patients with AD in the uncinate and inferior occipital fasciculi (Taoka et al., 2006), and in the corpus callosum and WM of the frontal, temporal, and parietal lobes (Bozzali et al., 2002). Two studies in AD (Head et al., 2004; Medina et al., 2006) demonstrated generalized alterations in diffusion measures of posterior lobar WM that differed from those seen in normal aging. Two recent studies provide preliminary investigation into mechanisms of WM alteration in AD through the examination of axial and radial diffusivity (Choi et al., 2005; Huang et al., 2007). These studies examined selected regions of interest in small participant samples (10 AD in the former, and 6 AD in the latter study), and reached different conclusions with one focusing on compromised myelin (Choi et al., 2005) and the other suggesting loss of axonal processes as a primary pathologic mechanism (Huang et al., 2007). These prior studies provide important information about the regional patterns of AD pathology, yet questions remain about the whole brain patterns of WM change in these various diffusion parameters in AD. Additionally, no prior study has examined how classically described measures of pathology such as white matter signal abnormalities and hippocampal atrophy contribute to the changes measured.

The current study aimed to elucidate regional patterns of alterations in diffusion parameters in AD through a comprehensive, whole brain analysis of commonly and recently described DTI measures of tissue integrity. These analyses included the examination of anisotropy and axial and radial diffusivity components, and whether changes in these diffusion parameters provide information beyond traditional MRI measures of gray and WM degeneration. We used recently developed procedures in the FSL image analysis suite (http://www.fmrib.ox.ac.uk/fsl/) for interparticipant registration, reducing potential confounds in spatial normalization. We additionally utilized tractography procedures to define a path of interest (POI) in the native space of each individual to confirm voxel-based results. We find complex regional patterns of alterations in diffusion parameters with AD, with prominent changes in pathways associated with

Table 1
Participant demographics

	OA	AD
N	54 (45 F/9 M)	20 (16 F/4 M)
Age	75.8 (5.6)	77.8 (4.9)
MMSE ($n=26$)	28.8 (1.2)[a]	20.0 (5.4)[d]
BDS ($n=49$)	0.86 (1.0)[b]	12.9 (6.4)
TICS ($n=22$)	34.4 (2.0)[c]	NA
CDR global ($n=20$)	NA	11 (.5)/7 (1)/2 (2)
CDR sum of boxes ($n=20$)	NA	4.9 (2.9)

Data presented as mean and standard deviation where applicable. MMSE, Mini Mental State Examination; BDS, Blessed Dementia Scale; TICS, Telephone Interview of Cognitive Status; CDR, Clinical Dementia Rating (Hughes et al., 1982; Morris, 1997); Higher scores indicate better performance on MMSE (0–30) and TICS (0–39), whereas lower scores indicate better performance on BDS (0–37), global CDR (0–3), and CDR sum of boxes (0–18).
[a] $n=20$.
[b] $n=29$.
[c] $n=22$.
[d] $n=6$.

the hippocampal formation. These changes are beyond what can be explained by classically described AD pathology, and suggest that multiple pathologies may disrupt the transfer of neocortical information to limbic structures important for a range of cognitive processes.

2. Methods

2.1. Participants

Images were obtained for 74 participants (Table 1). Twenty patients with probable Alzheimer's disease (mean age 77.8 ± 4.9 years) were recruited through the Massachusetts General Hospital Memory Disorders Unit (MGH-MDU) and 54 non-demented older adults (OA, mean age 75.8 ± 5.6 years) through the Harvard Cooperative Program on Aging (http://www.hebrewrehab.org/home institute.cfm?id=90) and the Nurses' Health Study (http://www.channing.harvard.edu/nhs/) at Harvard Medical School and Brigham and Women's Hospital. OA were screened for dementia using one of the following mental status examinations: the Mini Mental Status Exam (MMSE) (Folstein et al., 1975), the Blessed Dementia Scale (BDS) (Blessed et al., 1968; Stern et al., 1990), or the Telephone Interview of Cognitive Status (TICS) (de Jager et al., 2003; Lipton et al., 2003). AD patients were assessed by the Clinical Dementia Rating scale (CDR) (Hughes et al., 1982; Morris, 1997; Morris et al., 1997) which yields a calculated global score (CDR rating) as well as a summated score of individual CDR domains (sum of boxes). All patients with AD were assessed by a memory disorders neurologist from the MGH-MDU. AD diagnoses as determined by CDR score were very mild to mild AD in 90% and moderate dementia in 10%. Participants were excluded if they had a history of significant neurologic or psychiatric disorder (other than AD), or serious cerebrovascular conditions. Groups were matched for proportion of individuals with controlled elevated blood pressure.

2.2. DTI acquisition

Global and regional WM integrity was assessed using DTI measures of FA and diffusivity (comprised of axial and radial components (Budde et al., 2007; Song et al., 2002, 2003)), as well as through T2 image intensity measured through the B = 0 DTI volume. Image acquisition employed single shot echo planar imaging with a twice-refocused spin echo pulse sequence, optimized to minimize eddy current-induced image distortions (Reese et al., 2003) (Siemens Avanto; TR/TE = 7400/89 ms, $b = 700\ \mathrm{s\,mm^{-2}}$, 256 mm × 256 mm FOV, 128 × 128 matrix, 2 mm slice thickness with 0-mm gap, 10 T2 + 60 DWI, total acquisition time 8 min, 38 s). We acquired 64 slices in the AC-PC plane. The 60 diffusion weighted directions were obtained using the electrostatic shell method (Jones et al., 1999), providing a high signal-to-noise diffusion volume. The diffusion tensor was calculated on a voxel-by-voxel basis with conventional reconstruction methods (Basser et al., 1994) using tools developed at the Martinos Center at MGH.

2.3. DTI preprocessing and analysis: motion and eddy current correction

Image preprocessing was performed as described in our previous work (Salat et al., 2005a,b). Diffusion volumes were motion corrected and averaged using FLIRT (FMRIB's Linear Image Registration Tool; http://www.fmrib.ox.ac.uk/analysis/research/flirt/) (Jenkinson et al., 2002) with mutual information cost function to register each direction to the minimally eddy current distorted T2-weighted DTI volume that had no diffusion weighting.

2.4. Fractional anisotropy (FA) and diffusivity map calculation

The primary measures acquired from the DTI data were two common scalar metrics describing the WM microstructure. FA, which is dependent on the orientational coherence of the diffusion compartments within a voxel (Pierpaoli and Basser, 1996), was considered the primary metric of interest given the use of this parameter in a number of recent studies of tissue deterioration. FA was calculated using the standard formula defined previously (Basser, 1997). Diffusivity is a scalar measure of the total amount of diffusion within a voxel calculated as described in previous work (Basser and Pierpaoli, 1996). We additionally examined measures of axial (λ_1) and radial [$(\lambda_2 + \lambda_3)/2$] diffusivity as described in prior work (Budde et al., 2007; Song et al., 2002, 2003). T2 images were obtained using the exact parameters as the diffusion sensitive images except without any diffusion weighting. The T2 images were analyzed to determine whether changes

other than those in tissue microstructure contributed to the observed effects because T2 differences would reveal technical artifact such as image registration or atrophy, as well as large scale signal changes such as WM signal abnormalities (e.g. hyperintensities).

2.5. Nonlinear registration and tract-based spatial statistics (TBSS) (Rueckert et al., 1999; Smith et al., 2006; Smith et al., 2004)

Voxelwise statistical analysis of the FA data was carried out using TBSS (Tract-Based Spatial Statistics (Smith et al., 2006)), part of FSL (Smith et al., 2004). All participants' diffusion data were first aligned into a common space using the nonlinear registration IRTK (Rueckert et al., 1999) (http://www.doc.ic.ac.uk/∼dr/software). Next, a mean FA image was created across all participants, and this mean image was thinned to create a mean FA skeleton which represents the centers of all tracts common to the group. Each participant's aligned FA data were then projected onto this skeleton and the resulting data fed into voxelwise group statistics. Data along the skeleton were smoothed utilizing an anatomical constraint to limit the smoothing to neighboring data within adjacent voxels along the skeleton. All analyses were masked to only display regions with FA values of >0.2 to avoid examination of regions that are likely comprised of multiple tissue types or fiber orientations. The exact transformations derived for the anisotropy maps were applied to the T2 and diffusivity volumes for matched processing of all image volumes. Statistical maps were dilated from the TBSS skeleton for visualization purposes.

2.6. Hippocampal, WM, and WM signal abnormality volume measurements

Hippocampal, WM, and WM signal abnormality volume measurements were calculated through an automated procedure, using probabilistic information estimated from a manually labeled training set as described in our prior work (Fischl et al., 2002; Han et al., 2006; Walhovd et al., 2005). All volumetric measures were corrected as a percentage of intracranial volume (ICV).

2.7. POI analyses

We created highly constrained region of interest measures in parahippocampal WM across multiple participants using a procedure termed POI to reconstruct optimal pathways from a DTI image. This procedure was performed to obtain native space measurements across individuals in a homologous region of WM spanning the anterior to posterior parahippocampal gyrus. This region is comprised of multiple important fiber systems, including the perforant pathway, the parahippocampal/cingulum fibers, and fibers projecting from the amygdala to the parahippocampal region (the anatomy of the cortical projections recently summarized in (Mohedano-Moriano et al., 2007; Schmahmann and Pandya, 2006)). Anterior-posterior fiber systems dominate the tensor directionality in this region. However, it is important to note that additional fiber systems can contribute to the diffusion parameters of tissue integrity within this path. The POI was created by first transforming each participant's T2 and anisotropy maps to standardized space to facilitate identification of manually placed homologous initiation and termination points for the POI in each individual's DTI volume. Based on the tensor data, the optimal (strongest) path among all voxels in the labeled start and end points in the 3D volume was identified, and a path was created between those two points. FA was then sampled from the central voxels along the entire path, and the values were interpolated so that the number of samples along the path was the same across participants for point-by-point FA comparisons. Compared to region of interest approaches, the POI method allows sampling over extended WM pathways by simply specifying the initial and terminal points. The path construction algorithm is based on the replica exchange Monte Carlo (REMC) method (Habeck et al., 2005; Rieping et al., 2005; Swendsen and Wang, 1986), a recently developed improvement to the Metropolis–Hastings algorithm. The REMC algorithm operates by simulating multiple replica of the system simultaneously. Each system undergoes optimization according to the classical Metropolis–Hastings procedure, but the different replica can exchange temperatures through a Metropolis step. The multiple replica can search the configuration space efficiently, and the temperature exchange step enables the replica to overcome local minima. The REMC algorithm models the WM pathway as a trilinear spline with a sparse number of control points. The energy of the path is defined as the negative log product integral of the diffusion orientation distribution function (Tuch, 2004) along the path (Fig. 4). Data were smoothed using an anatomical constraint along the path by obtaining the mean of each set of three neighboring voxels.

3. Results

3.1. Voxel-based group comparisons of DTI measures

Fig. 1 demonstrates a coronal slice showing the mean FA map of each group from the spatially normalized FA volumes using the IRTK nonlinear registration step (Rueckert et al., 1999) of the tract-based spatial statistics (TBSS) (Smith et al., 2006) procedure (top), and a representative individual FA map (bottom) from the OA (left) and the AD (right) groups. Importantly, much of the anatomic detail of the individual participant volumes was retained in this initial processing of the TBSS procedure.

Table 2 lists regions showing reduced FA in AD compared to OA without the use of any nuisance regressors. FA was reduced in numerous regions including bilateral reductions in lateral occipital WM, middle and inferior temporal

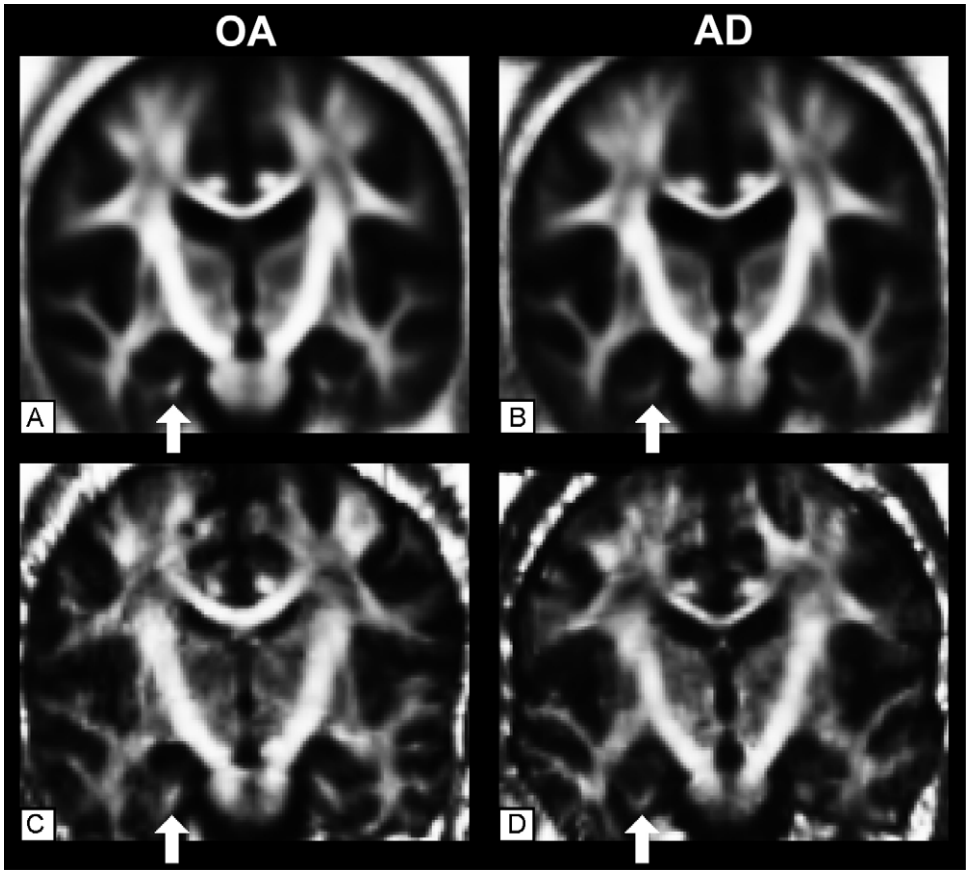

Fig. 1. Top panel. Example of a mean FA map in non-demented older adults (A) and patients with AD (B) resulting from the spatial normalization of the FA volumes using the IRTK nonlinear registration procedure (Rueckert et al., 1999) (http://www.doc.ic.ac.uk/~dr/software) from tract-based spatial statistics (TBSS) (Smith et al., 2006). Bottom panel. Example of an individual FA map in a non-demented older adult (C) and in a patient with AD (D). Importantly, much of the anatomic detail in the individual participant volumes is retained in the group averaged volumes, and these averages do not qualitatively differ substantially between the control and AD groups, demonstrating the robustness of the nonlinear procedure. Alterations in parahippocampal FA can be qualitatively seen in the group average as well as in the individual participant comparison (reduced FA intensity between groups at the white arrows).

WM, inferior parietal/supramarginal WM, precuneus WM, and parahippocampal WM. Fig. 2 demonstrates the TBSS-based statistical comparison of FA and diffusivity between OA and AD controlling for T2 intensity at each voxel (Fig. 2, panel A). When controlling for T2 intensity, changes in FA were most prominent in parahippocampal and temporal, precuneus, and ventromedial frontal WM (Fig. 2). Diffusivity increased with AD in regions similar to those reported for FA yet were somewhat more widespread with additional changes in the corpus callosum, cingulum, occipital, and periventricular regions. Overlap in FA and diffusivity changes (results with a p value <0.01) was greatest in medial temporal, precuneus, and ventromedial frontal WM (Fig. 2; bottom left panel). Analyses in Fig. 2 controlled for T2 intensity at each voxel, and therefore the changes measured exceeded those of T2 which would be affected by partial volume and WM hyperintensities.

Increases were apparent in the radial as well as axial components of diffusivity (Fig. 2, panel B) however, these components were affected in an almost completely regionally distinct manner. Increases in axial diffusivity were most apparent in periventricular, occipital, and callosal regions whereas increases in radial diffusivity were more selectively localized to medial temporal, occipital, and precuneus WM. Overlap of changes in the two components was in small portions of occipital and temporal WM (Fig. 2, right panel, bottom).

3.2. Comparisons of DTI measures controlling for hippocampal volume and T2

Because hippocampal atrophy is a neuroimaging hallmark (although not perfectly specific) of AD degenerative processes (Jack et al., 1992), we next examined whether changes in the diffusion measures remained when controlling for hippocampal volume in addition to T2 intensity. Controlling for these parameters reduced the statistical effect on FA and diffusivity in certain areas including the precuneus and medial frontal WM (Fig. 3). However, the statistical effect on temporal lobe WM, and in particular, temporal and parahippocampal WM remained. Differences in thalamic and internal capsule WM were also highlighted in this analysis. Overlap in changes in FA and in diffusivity was apparent in medial temporal, thalamic, and temporal stem and pyrami-

Table 2
Regions of altered FA in AD

Region	Size (mm^3)	Minimum p value (10^{-x})	Weight[a]
Temporal			
Lh-inferior/middle temporal	1467	5.81	8523.30
Lh-parahippocampal	534	5.41	2888.90
Rh-middle temporal	502	4.75	2384.50
Rh-fusiform/inferior temporal/middle temporal	579	3.81	2206.00
Lh-medial temporal pole	358	4.66	1668.30
Lh-middle temporal	270	4.70	1269.00
Rh-temporal stem	304	3.28	997.12
Rh-inferior temporal	204	4.16	848.64
Rh-inferior temporal	181	3.97	718.57
Rh-middle temporal	170	3.98	676.60
Rh-parahippocampal	131	4.44	581.64
Lh-fusiform	161	−3.43	552.23
Lh-parahippocampal	87	3.71	322.77
Parietal			
Lh-precuneus	1219	4.18	5095.40
Lh-inferior parietal	620	4.74	2938.80
Lh-inferiorparietal/supramarginal	446	4.80	2140.80
Rh-supramarginal	366	3.59	1313.90
Lh-cuneus/precuneus	274	4.69	1285.10
Rh-precuneus	343	3.32	1138.80
Rh-inferior parietal	231	4.03	930.93
Lh-inferior parietal	176	4.48	788.48
Rh-precuneus	108	3.16	341.28
Lh-inferior parietal	109	3.07	334.63
Lh-precuneus	90	3.62	325.80
Frontal			
Rh-medial/lateral orbitofrontal	421	3.71	1561.90
Rh-superior frontal	181	4.30	778.30
Lh-rostral middle frontal	89	3.66	325.74
Occipital			
Lh-lateral occipital/lingual	851	4.58	3897.60
Rh-lateraloccipital	516	5.78	2982.50
Deep/other			
Lh-periventricular	1046	−5.00	5230.00
Lh-pulvinar	433	5.68	2459.40
Fornix	269	4.73	1272.40
Lh-anterior callosum	271	3.04	823.84
Rh-anterior capsule	210	3.02	634.20
Rh-pulvinar	133	4.71	626.43
Lh-posterior callosum	151	3.16	477.16
Rh-cerebellum	97	4.21	408.37
Lh-ventral diencephalon	83	3.80	315.40

Clusters with a p value of ≤ 0.01 and a cluster size >40 voxels.

[a] Regions were ordered by region/lobe and by a weighting calculated as the product of the cluster size by the minimum p value (expressed as 10^{-x}). The final weighting was somewhat arbitrary due to specifics of the processing procedures. Clusters with <300 weight were omitted from the table. Regional definitions were based on proximity to neural labels described in (Desikan et al., 2006; Fischl et al., 2002).

dal WM when controlling for T2 and hippocampal volume. These results demonstrate that diffusion measures in these regions provide unique information compared to hippocampal volume and T2 signal intensity alone.

3.3. POI analysis

The results of the voxel-based analyses in parahippocampal WM were confirmed using the POI tractography technique to extract native space values from each individual. Fig. 4 demonstrates this procedure and results from this analysis. FA was reduced in patients on a point-by-point basis along the majority of the path, confirming the findings from the voxel-based results with stronger effects in the more anterior portions of the pathway (the points on the right side of the plot; bottom panel). Total path length did not significantly differ between the two groups. Mean values of all points from along the path demonstrated highly significant reduction in FA (Fig. 5). For comparison, the effects of AD on hippocampal volume, whole brain WM volume, and white matter signal

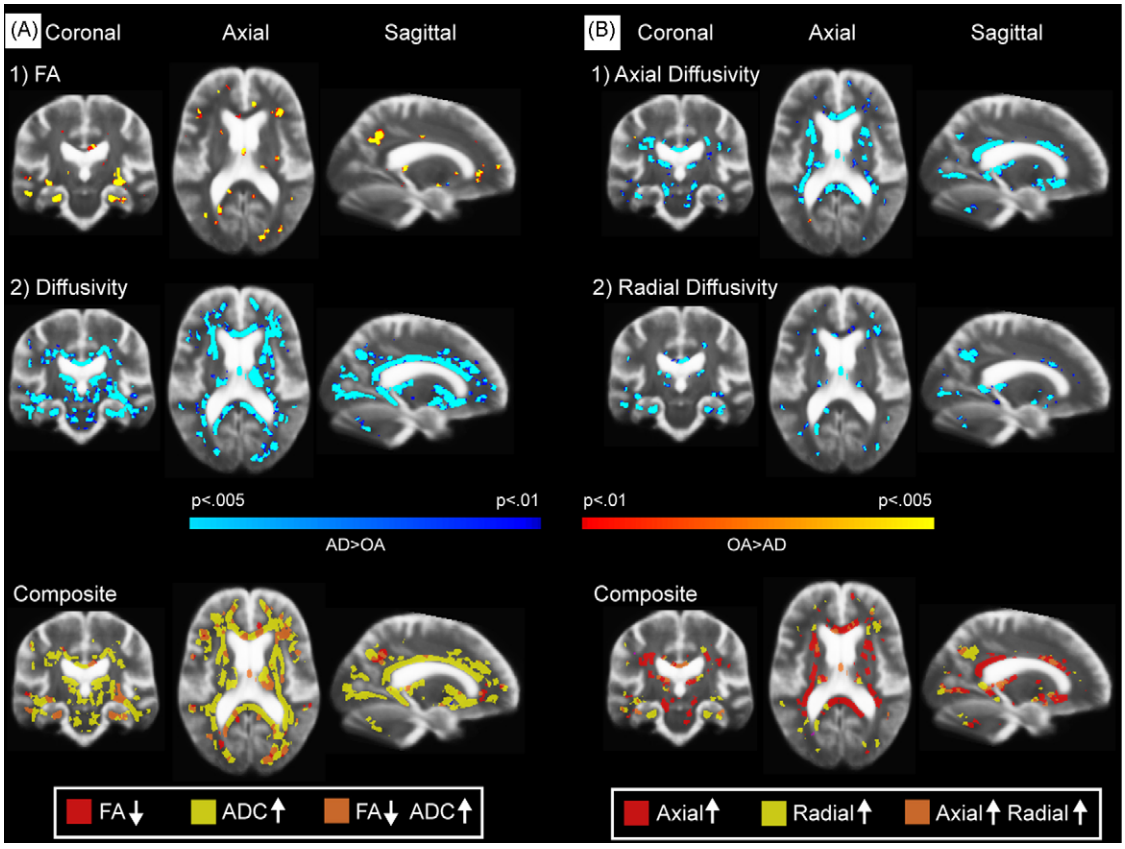

Fig. 2. TBSS-based statistical comparison of FA and diffusivity between OA and AD, regressing out T2 signal intensity. Left panel. When controlling for T2 intensity, changes in FA were most prominent in parahippocampal, temporal, precuneus, and ventromedial frontal WM. Diffusivity increased with AD in regions similar to those reported for FA yet somewhat more widespread with additional changes in the corpus callosum, cingulum, occipital, and periventricular regions. Composite map of the statistical patterns of diffusion changes with group comparisons (bottom panel). Classes were distinguished based on the unique combination of each direction of the statistical results for each map for any results with a p value of 0.01 or lower (i.e. an increase or a decrease [two classes] in FA or diffusivity and each potential unique combination of classes). Overlap in FA and diffusivity changes was greatest in medial temporal, precuneus, and ventromedial frontal WM (bottom left panel). Analyses controlled for T2 intensity at each voxel, and therefore the changes measured exceeded those of T2 which would be affected by partial volume and/or WM hyperintensities. Right panel. Alterations in axial (right top) and radial (right middle) diffusivity in AD, and the composite of these effects (right bottom).

abnormality volume (Fischl et al., 2002; Han et al., 2006; Walhovd et al., 2005) are also presented (Fig. 5).

4. Discussion

These data demonstrate for the first time, the distinct and overlapping anatomy of whole brain changes in anisotropy and diffusivity, as well as the differential patterns of alterations in axial and radial diffusivity. These different diffusion parameters provide unique information, and the results demonstrate the complex anatomical basis of DTI changes in AD. To a certain extent, the most prominent regional tissue changes in overlapping diffusion parameters resembled the anatomic connectivity of MTL structures that are important for memory processes, with alterations in parahippocampal and ventromedial frontal WM. Of note were bilateral alterations in FA in the precuneus, which is connected to the MTL by way of retrosplenial cortex, and is considered by some to be part of the limbic system (Cavanna and Trimble, 2006). This region is of great current interest in the study of AD because the precuneus is likely an extension of the MTL memory system (Vincent et al., 2006), and is functionally and structurally altered by AD pathology (Hirono et al., 2004; Ishii et al., 2005; Lustig et al., 2003; Mintun et al., 2006; Rombouts et al., 2005; Wang et al., 2006). Several regions outside of this medial temporal network were also affected, however, including various portions of occipital, temporal, and parietal WM, and more minimal changes in frontal WM. Greater changes in radial compared to axial diffusivity were apparent in the parahippocampal WM, suggesting that the pathology in this region includes some form of myelin degradation and the current data demonstrate the first whole brain regional description of this effect.

Prior voxel-based morphometry studies have demonstrated alterations in parahippocampal WM in AD (Stoub et al., 2006). Our work is also in accord with previous work demonstrating altered diffusion properties in parahippocampal, thalamic, and cingulate WM (Rose et al., 2006) and in

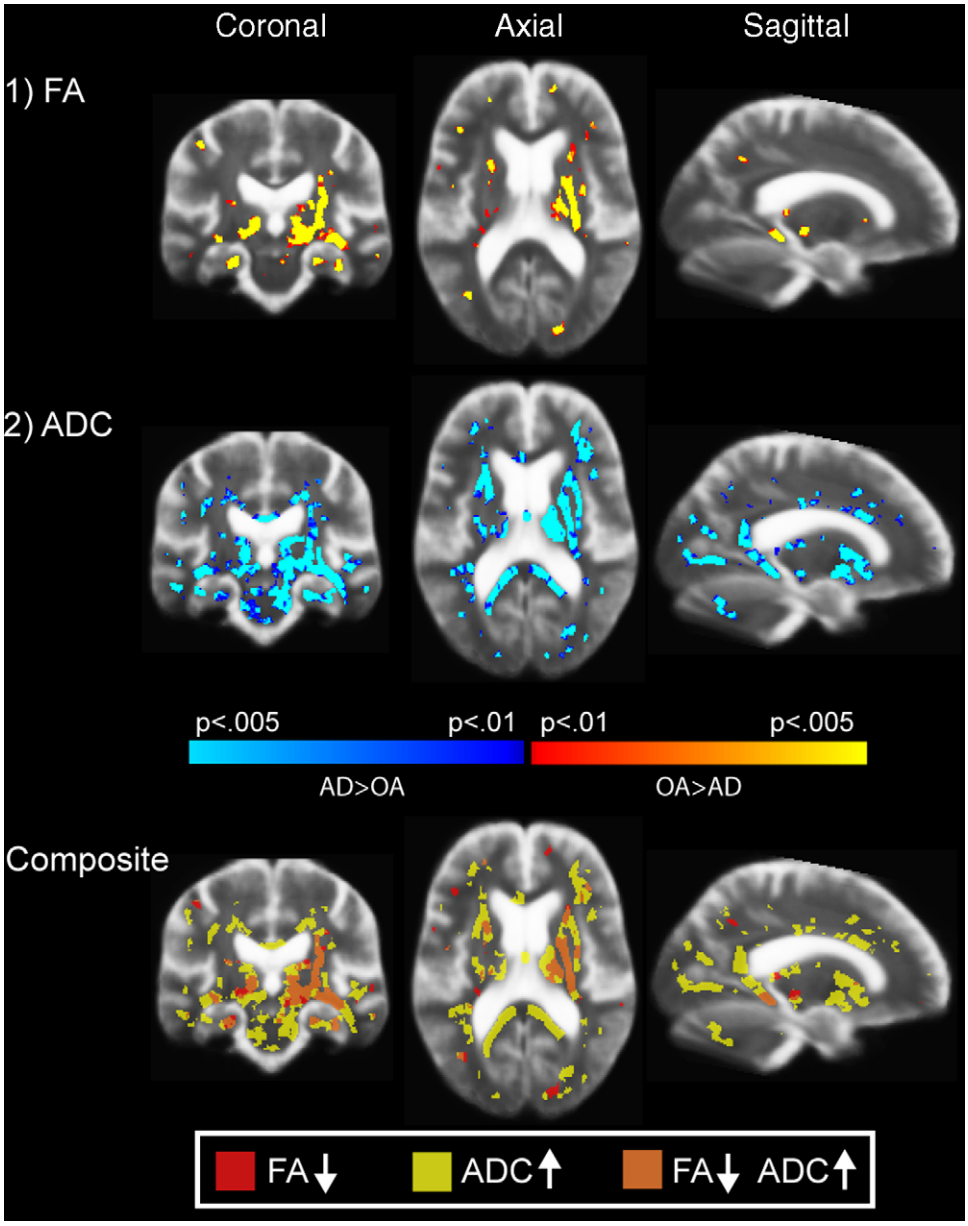

Fig. 3. TBSS-based statistical comparison of FA and diffusivity between OA and AD, regressing out T2 signal intensity and hippocampal volume. Hippocampal volume was treated as a nuisance covariate to determine whether there were effects of AD on diffusion parameters that were independent of this classical imaging measure of AD pathology. FA reductions with AD were prominent in medial temporal, temporal stem, and thalamic regions (top panel). Diffusivity changes were apparent throughout a number of ventral and periventricular WM areas (middle panel). Composite map of FA and diffusivity changes was greatest in temporal WM (bottom panel). Because hippocampal volume and T2 were both treated as nuisance covariates, these results demonstrate the unique variance in diffusion parameters that is not explained by these other types of pathologic changes.

posterior lobar WM (Head et al., 2004; Medina et al., 2006) in individuals with AD and mild cognitive impairment, suggesting that the changes measured here could be apparent in the earliest stages of AD. Rose and colleagues (Rose et al., 2006) suggested that changes in the left hemisphere were greater than those in the right hemisphere. These results are qualitatively supported by the POI analyses in the current study, demonstrating that although left and right parahippocampal WM are both affected in AD, the left path demonstrated more points reaching a statistical effect compared to the homologous region in the right hemisphere. Formal testing for laterality effects will be an important topic of future research. Additionally, the POI analyses suggest a potential anterior to posterior gradient of WM damage in the parahippocampal WM. Such a finding would have important implications for memory function as it is suggested that recollection, familiarity, and novelty are supported by different MTL subregions (Daselaar et al., 2006). These data are also in accord with regional patterns recently presented in a study contrasting AD and cerebrovascular disease (Chen et al., 2007). Altered DTI

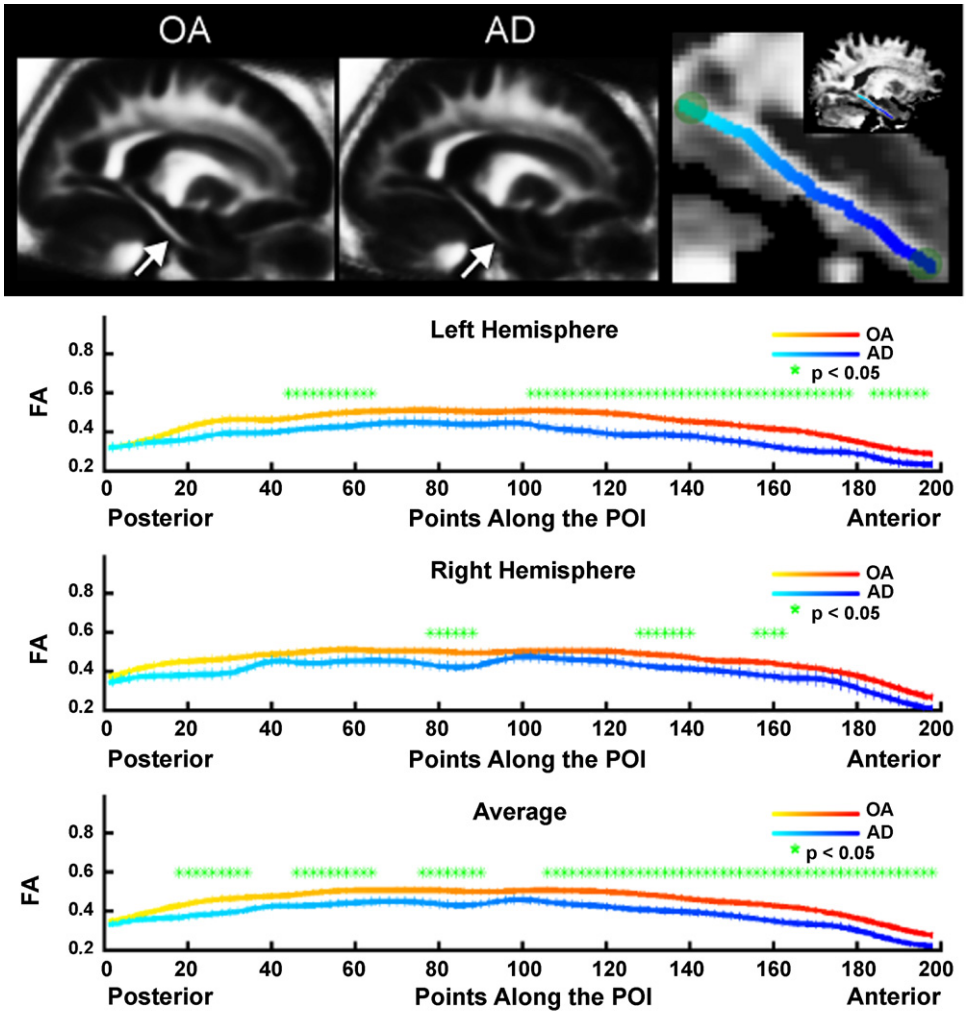

Fig. 4. Demonstration of the POI technique and analysis of parahippocampal WM. Seed points were manually placed in each individual participant's diffusion volumes at anterior and posterior points in the parahippocampal WM defined by morphometric landmarks in the T2 image. Those points were then connected using the optimal path calculated from the diffusion tensor information (top panel; see Section 2). The mean of the OA (top left) and AD (top middle) of a single sagittal slice is presented to demonstrate the visual differences in the raw data between these groups (arrows). FA was sampled from the central voxels along the path, providing an individual POI for each participant, and minimizing the potential confounds of partial volume contamination from more peripheral voxels. FA was most affected in anterior portions of the parahippocampal WM, but significant reductions in FA were found with AD along the majority of the path when the mean FA across the hemispheres was examined (bottom plot). Overall path length did not differ between the groups.

measures have been related to indices of disease severity and cognitive ability, with particular association with episodic memory, presenting a potential role for DTI in uncovering WM degeneration in the clinical presentation of AD (Rose et al., 2006). The present results demonstrate regional changes in parahippocampal and precuneus WM, and degeneration of these regions may result in isolation of the hippocampus from neocortical input and related areas that have been recently described to comprise part of a functional memory circuit (Vincent et al., 2006).

The relation between DTI measures and more classical imaging indices of pathology, including brain volume, is not clear. Our prior volumetric work demonstrated significantly lower prefrontal WM volume in patients with AD compared to age-matched control participants (Salat et al., 1999a), and the current data may suggest that this effect is due to degenerative changes in selective regions. The current data demonstrate that changes in diffusion metrics provide independent information beyond hippocampal volume alone. Removing variance due to hippocampal volume did not reduce the effects measured in parahippocampal WM, and even highlighted effects in thalamic regions that were less apparent in the group comparisons without consideration of hippocampal volume. The association between microstructural FA measures and macrostructural volumetric measures may be complex (Salat et al., 2005b). Similarly, the pathologic basis of changes in DTI measures is currently unknown. Prior studies report loss of oligodendrocytes, reactive astrocytosis, and reduction in neuropil density that could contribute to WM damage in AD (Sjobeck et al., 2006), and we posit that at least some of the measured effects could be due to Wallerian degeneration of axons and the surrounding myelin

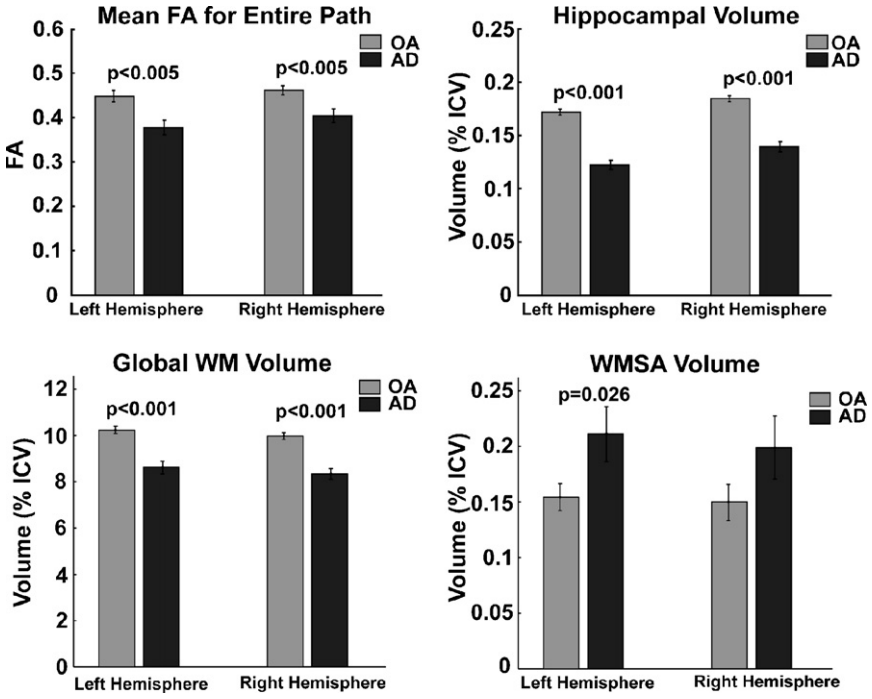

Fig. 5. Mean anisotropy along the entire path (top left) differed between OA and AD in the left and right hemispheres. For comparison, traditional imaging measures of AD pathology are presented including hippocampal volume (top right), total WM volume (bottom left), and white matter signal abnormality (WMSA; bottom right) volume.

sheath. However, the fact that effects remained in the MTL WM after regressing out hippocampal volume and that there was greater alteration in radial as opposed to axial diffusivity in parahippocampal WM supports prior work demonstrating reduced myelin staining in AD (Hyman et al., 1986), and suggests that the effects measured are somewhat independent of regional cortical degeneration and may represent a unique myelin pathology (Budde et al., 2007; Song et al., 2002, 2003). These findings should be interpreted with caution however, as it is important to note that the current data also demonstrated a regional increase in axial diffusivity. This is not what is expected from the animal models demonstrating that axonal pathology should result in a decrease in axial diffusivity (Song et al., 2003), and little information exists for the interpretation of increased axial diffusivity. DTI has been used to guide pathology studies (Englund et al., 2004), and further work with similar methods will likely yield important new information about how these novel diffusion measures relate to histopathology in AD.

The current results have some limitations. The changes in FA measured were relatively small and regionally localized, and thus it is unknown how early such changes could be detected. Future work will examine individuals with mild cognitive impairment to determine whether the current pattern of results exists in preclinical stages of disease. Although advanced procedures were applied to address common concerns of diffusion imaging studies, further improvement is required in this field. Methods to enhance spatial (Li et al., 2005; Liu et al., 2004, 2005) and angular (Tuch, 2004; Tuch et al., 2002) resolution will be necessary to fully exclude concerns about eddy current and susceptibility artifact distortions. Similarly, although the procedures used here are superior to standard linear transformations for registration of DTI data, the potential still exists for further refinement of DTI registration using the full tensor information (Park et al., 2003). In spite of these limitations, the current analysis procedures provide a set of techniques that address common concerns for the analysis of DTI data, and demonstrate the vulnerability of WM to AD pathology. Thus, along with cortical degeneration, we suggest that an additional mechanism underlying AD clinical symptoms is the WM degeneration that further isolates MTL structures.

Acknowledgements

This work was supported in part by NIH K01AG024898, a Massachusetts Alzheimer's Disease Research Center Pilot Grant 2001/2002 (AG05886), the National Center for Research Resources (P41RR14075), the Mental Illness and Neuroscience Discovery (MIND) Institute, and a grant from the National Alliance for Medical Image Computing (NAMIC U54 EB05149). We thank Dr. Francine Grodstein and the Nurses' Health Study for a portion of the participant recruitment and imaging.

References

Au, R., Massaro, J.M., Wolf, P.A., Young, M.E., Beiser, A., Seshadri, S., D'Agostino, R.B., DeCarli, C., 2006. Association of white matter hyper-

intensity volume with decreased cognitive functioning: the Framingham Heart Study. Arch. Neurol. 63 (2), 246–250.

Ball, M.J., 1978. Topographic distribution of neurofibrillary tangles and granulovacuolar degeneration in hippocampal cortex of aging and demented patients. A quantitative study. Acta Neuropathol. (Berl.) 42 (2), 73–80.

Basser, P.J., 1995. Inferring microstructural features and the physiological state of tissues from diffusion-weighted images. NMR Biomed. 8 (7–8), 333–344.

Basser, P.J., 1997. New histological and physiological stains derived from diffusion-tensor MR images. Ann. N. Y. Acad. Sci. 820, 123–138.

Basser, P.J., Mattiello, J., LeBihan, D., 1994. Estimation of the effective self-diffusion tensor from the NMR spin echo. J. Magn. Reson. B 103 (3), 247–254.

Basser, P.J., Pierpaoli, C., 1996. Microstructural and physiological features of tissues elucidated by quantitative-diffusion-tensor MRI. J. Magn. Reson. B 111 (3), 209–219.

Blessed, G., Tomlinson, B.E., Roth, M., 1968. The association between quantitative measures of dementia and of senile change in the cerebral grey matter of elderly subjects. Br. J. Psychiatry 114 (512), 797–811.

Bozzali, M., Falini, A., Franceschi, M., Cercignani, M., Zuffi, M., Scotti, G., Comi, G., Filippi, M., 2002. White matter damage in Alzheimer's disease assessed in vivo using diffusion tensor magnetic resonance imaging. J. Neurol. Neurosurg. Psychiatry 72 (6), 742–746.

Braak, H., Braak, E., 1991. Neuropathological stageing of Alzheimer-related changes. Acta Neuropathol. (Berl.) 82 (4), 239–259.

Brun, A., Englund, E., 1986. A white matter disorder in dementia of the Alzheimer type: a pathoanatomical study. Ann. Neurol. 19 (3), 253–262.

Budde, M.D., Kim, J.H., Liang, H.F., Schmidt, R.E., Russell, J.H., Cross, A.H., Song, S.K., 2007. Toward accurate diagnosis of white matter pathology using diffusion tensor imaging. Magn. Reson. Med. 57 (4), 688–695.

Cavanna, A.E., Trimble, M.R., 2006. The precuneus: a review of its functional anatomy and behavioural correlates. Brain 129 (Pt 3), 564–583.

Chen, S.Q., Kang, Z., Hu, X.Q., Hu, B., Zou, Y., 2007. Diffusion tensor imaging of the brain in patients with Alzheimer's disease and cerebrovascular lesions. J. Zhejiang Univ. Sci. B 8 (4), 242–247.

Choi, S.J., Lim, K.O., Monteiro, I., Reisberg, B., 2005. Diffusion tensor imaging of frontal white matter microstructure in early Alzheimer's disease: a preliminary study. J. Geriatr. Psychiatry Neurol. 18 (1), 12–19.

Daselaar, S.M., Fleck, M.S., Cabeza, R., 2006. Triple dissociation in the medial temporal lobes: recollection, familiarity, and novelty. J. Neurophysiol. 96 (4), 1902–1911.

de Jager, C.A., Budge, M.M., Clarke, R., 2003. Utility of TICS-M for the assessment of cognitive function in older adults. Int. J. Geriatr. Psychiatry 18 (4), 318–324.

de Leeuw, F.E., Korf, E., Barkhof, F., Scheltens, P., 2006. White matter lesions are associated with progression of medial temporal lobe atrophy in Alzheimer disease. Stroke 37 (9), 2248–2252.

Desikan, R.S., Segonne, F., Fischl, B., Quinn, B.T., Dickerson, B.C., Blacker, D., Buckner, R.L., Dale, A.M., Maguire, R.P., Hyman, B.T., Albert, M.S., Killiany, R.J., 2006. An automated labeling system for subdividing the human cerebral cortex on MRI scans into gyral based regions of interest. Neuroimage 31 (3), 968–980.

Englund, E., Brun, A., 1990. White matter changes in dementia of Alzheimer's type: the difference in vulnerability between cell compartments. Histopathology 16 (5), 433–439.

Englund, E., Brun, A., Alling, C., 1988. White matter changes in dementia of Alzheimer's type. Biochemical and neuropathological correlates. Brain 111 (Pt6), 1425–1439.

Englund, E., Sjobeck, M., Brockstedt, S., Latt, J., Larsson, E.M., 2004. Diffusion tensor MRI post mortem demonstrated cerebral white matter pathology. J. Neurol. 251 (3), 350–352.

Fischl, B., Salat, D.H., Busa, E., Albert, M., Dieterich, M., Haselgrove, C., van der Kouwe, A., Killiany, R., Kennedy, D., Klaveness, S., Montillo, A., Makris, N., Rosen, B., Dale, A.M., 2002. Whole brain segmentation: automated labeling of neuroanatomical structures in the human brain. Neuron 33 (3), 341–355.

Folstein, M.F., Folstein, S.E., McHugh, P.R., 1975. "Mini-mental state" A practical method for grading the cognitive state of patients for the clinician. J. Psychiatr Res. 12 (3), 189–198.

Fotenos, A.F., Snyder, A.Z., Girton, L.E., Morris, J.C., Buckner, R.L., 2005. Normative estimates of cross-sectional and longitudinal brain volume decline in aging and AD. Neurology 64 (6), 1032–1039.

Gomez-Isla, T., Price, J.L., McKeel Jr., D.W., Morris, J.C., Growdon, J.H., Hyman, B.T., 1996. Profound loss of layer II entorhinal cortex neurons occurs in very mild Alzheimer's disease. J. Neurosci. 16 (14), 4491–4500.

Habeck, M., Nilges, M., Rieping, W., 2005. Replica-exchange Monte Carlo scheme for Bayesian data analysis. Phys. Rev. Lett. 94 (1), 018105.

Han, X., Jovicich, J., Salat, D., van der Kouwe, A., Quinn, B., Czanner, S., Busa, E., Pacheco, J., Albert, M., Killiany, R., Maguire, P., Rosas, D., Makris, N., Dale, A., Dickerson, B., Fischl, B., 2006. Reliability of MRI-derived measurements of human cerebral cortical thickness: the effects of field strength, scanner upgrade and manufacturer. Neuroimage 32 (1), 180–194.

Head, D., Buckner, R.L., Shimony, J.S., Williams, L.E., Akbudak, E., Conturo, T.E., McAvoy, M., Morris, J.C., Snyder, A.Z., 2004. Differential vulnerability of anterior white matter in nondemented aging with minimal acceleration in dementia of the Alzheimer type: evidence from diffusion tensor imaging. Cereb. Cortex 14 (4), 410–423.

Hirono, N., Hashimoto, M., Ishii, K., Kazui, H., Mori, E., 2004. One-year change in cerebral glucose metabolism in patients with Alzheimer's disease. J. Neuropsychiatry Clin. Neurosci. 16 (4), 488–492.

Hirono, N., Kitagaki, H., Kazui, H., Hashimoto, M., Mori, E., 2000. Impact of white matter changes on clinical manifestation of Alzheimer's disease: a quantitative study. Stroke 31 (9), 2182–2188.

Huang, J., Friedland, R.P., Auchus, A.P., 2007. Diffusion tensor imaging of normal-appearing white matter in mild cognitive impairment and early Alzheimer disease: preliminary evidence of axonal degeneration in the temporal lobe. AJNR Am. J. Neuroradiol. 28 (10), 1943–1948.

Hughes, C.P., Berg, L., Danziger, W.L., Coben, L.A., Martin, R.L., 1982. A new clinical scale for the staging of dementia. Br. J. Psychiatry 140, 566–572.

Hyman, B.T., Van Hoesen, G.W., Damasio, A.R., Barnes, C.L., 1984. Alzheimer's disease: cell-specific pathology isolates the hippocampal formation. Science 225 (4667), 1168–1170.

Hyman, B.T., Van Hoesen, G.W., Kromer, L.J., Damasio, A.R., 1986. Perforant pathway changes and the memory impairment of Alzheimer's disease. Ann. Neurol. 20 (4), 472–481.

Ishii, K., Kawachi, T., Sasaki, H., Kono, A.K., Fukuda, T., Kojima, Y., Mori, E., 2005. Voxel-based morphometric comparison between early- and late-onset mild Alzheimer's disease and assessment of diagnostic performance of z score images. AJNR Am. J. Neuroradiol. 26 (2), 333–340.

Jack Jr., C.R., Petersen, R.C., O'Brien, P.C., Tangalos, E.G., 1992. MR-based hippocampal volumetry in the diagnosis of Alzheimer's disease. Neurology 42 (1), 183–188.

Jenkinson, M., Bannister, P., Brady, M., Smith, S., 2002. Improved optimization for the robust and accurate linear registration and motion correction of brain images. Neuroimage 17 (2), 825–841.

Jernigan, T.L., Salmon, D.P., Butters, N., Hesselink, J.R., 1991. Cerebral structure on MRI. Part II: Specific changes in Alzheimer's and Huntington's diseases. Biol. Psychiatry 29 (1), 68–81.

Jones, D.K., Horsfield, M.A., Simmons, A., 1999. Optimal strategies for measuring diffusion in anisotropic systems by magnetic resonance imaging. Magn. Reson. Med. 42 (3), 515–525.

Li, T.Q., Kim, D.H., Moseley, M.E., 2005. High-resolution diffusion-weighted imaging with interleaved variable-density spiral acquisitions. J. Magn. Reson. Imaging 21 (4), 468–475.

Lipton, R.B., Katz, M.J., Kuslansky, G., Sliwinski, M.J., Stewart, W.F., Verghese, J., Crystal, H.A., Buschke, H., 2003. Screening for demen-

tia by telephone using the memory impairment screen. J. Am. Geriatr. Soc. 51 (10), 1382–1390.
Liu, C., Bammer, R., Kim, D.H., Moseley, M.E., 2004. Self-navigated interleaved spiral (SNAILS): application to high-resolution diffusion tensor imaging. Magn. Reson. Med. 52 (6), 1388–1396.
Liu, C., Moseley, M.E., Bammer, R., 2005. Simultaneous phase correction and SENSE reconstruction for navigated multi-shot DWI with non-Cartesian k-space sampling. Magn. Reson. Med. 54 (6), 1412–1422.
Lustig, C., Snyder, A.Z., Bhakta, M., O'Brien, K.C., McAvoy, M., Raichle, M.E., Morris, J.C., Buckner, R.L., 2003. Functional deactivations: change with age and dementia of the Alzheimer type. Proc. Natl. Acad. Sci. U. S. A. 100 (24), 14504–14509.
Medina, D., DeToledo-Morrell, L., Urresta, F., Gabrieli, J.D., Moseley, M., Fleischman, D., Bennett, D.A., Leurgans, S., Turner, D.A., Stebbins, G.T., 2006. White matter changes in mild cognitive impairment and AD: a diffusion tensor imaging study. Neurobiology. Aging 27 (5), 663–672.
Mintun, M.A., Larossa, G.N., Sheline, Y.I., Dence, C.S., Lee, S.Y., Mach, R.H., Klunk, W.E., Mathis, C.A., DeKosky, S.T., Morris, J.C., 2006. [11C]PIB in a nondemented population: potential antecedent marker of Alzheimer disease. Neurology 67 (3), 446–452.
Mohedano-Moriano, A., Pro-Sistiaga, P., Arroyo-Jimenez, M.M., Artacho-Perula, E., Insausti, A.M., Marcos, P., Cebada-Sanchez, S., Martinez-Ruiz, J., Munoz, M., Blaizot, X., Martinez-Marcos, A., Amaral, D.G., Insausti, R., 2007. Topographical and laminar distribution of cortical input to the monkey entorhinal cortex. J. Anat. 211 (2), 250–260.
Morris, J.C., 1997. Clinical dementia rating: a reliable and valid diagnostic and staging measure for dementia of the Alzheimer type. Int. Psychogeriatr. 9 (Suppl. 1), 173–176, discussion 7–8.
Morris, J.C., Ernesto, C., Schafer, K., Coats, M., Leon, S., Sano, M., Thal, L.J., Woodbury, P., 1997. Clinical dementia rating training and reliability in multicenter studies: the Alzheimer's Disease Cooperative Study experience. Neurology 48 (6), 1508–1510.
Moseley, M., 2002. Diffusion tensor imaging and aging—a review. NMR Biomed. 15 (7–8), 553–560.
Mungas, D., Harvey, D., Reed, B.R., Jagust, W.J., DeCarli, C., Beckett, L., Mack, W.J., Kramer, J.H., Weiner, M.W., Schuff, N., Chui, H.C., 2005. Longitudinal volumetric MRI change and rate of cognitive decline. Neurology 65 (4), 565–571.
Park, H.J., Kubicki, M., Shenton, M.E., Guimond, A., McCarley, R.W., Maier, S.E., Kikinis, R., Jolesz, F.A., Westin, C.F., 2003. Spatial normalization of diffusion tensor MRI using multiple channels. Neuroimage 20 (4), 1995–2009.
Pfefferbaum, A., Adalsteinsson, E., Sullivan, E.V., 2005. Frontal circuitry degradation marks healthy adult aging: Evidence from diffusion tensor imaging. Neuroimage 26 (3), 891–899.
Pfefferbaum, A., Sullivan, E.V., 2003. Increased brain white matter diffusivity in normal adult aging: relationship to anisotropy and partial voluming. Magn. Reson. Med. 49 (5), 953–961.
Pfefferbaum, A., Sullivan, E.V., Hedehus, M., Lim, K.O., Adalsteinsson, E., Moseley, M., 2000. Age-related decline in brain white matter anisotropy measured with spatially corrected echo-planar diffusion tensor imaging. Magn. Reson. Med. 44 (2), 259–268.
Pierpaoli, C., Basser, P.J., 1996. Toward a quantitative assessment of diffusion anisotropy. Magn. Reson. Med. 36 (6), 893–906.
Prins, N.D., van Dijk, E.J., den Heijer, T., Vermeer, S.E., Koudstaal, P.J., Oudkerk, M., Hofman, A., Breteler, M.M., 2004. Cerebral white matter lesions and the risk of dementia. Arch. Neurol. 61 (10), 1531–1534.
Reese, T.G., Heid, O., Weisskoff, R.M., Wedeen, V.J., 2003. Reduction of eddy-current-induced distortion in diffusion MRI using a twice-refocused spin echo. Magn. Reson. Med. 49 (1), 177–182.
Rieping, W., Habeck, M., Nilges, M., 2005. Inferential structure determination. Science 309 (5732), 303–306.
Rombouts, S.A., Barkhof, F., Goekoop, R., Stam, C.J., Scheltens, P., 2005. Altered resting state networks in mild cognitive impairment and mild Alzheimer's disease: an fMRI study. Hum. Brain Mapp. 26 (4), 231–239.
Rose, S.E., Chen, F., Chalk, J.B., Zelaya, F.O., Strugnell, W.E., Benson, M., Semple, J., Doddrell, D.M., 2000. Loss of connectivity in Alzheimer's disease: an evaluation of white matter tract integrity with colour coded MR diffusion tensor imaging. J. Neurol. Neurosurg. Psychiatry 69 (4), 528–530.
Rose, S.E., McMahon, K.L., Janke, A.L., O'Dowd, B., de Zubicaray, G., Strudwick, M.W., Chalk, J.B., 2006. Diffusion indices on magnetic resonance imaging and neuropsychological performance in amnestic mild cognitive impairment. J. Neurol. Neurosurg. Psychiatry 77 (10), 1122–1128.
Rueckert, D., Sonoda, L.I., Hayes, C., Hill, D.L., Leach, M.O., Hawkes, D.J., 1999. Nonrigid registration using free-form deformations: application to breast MR images. IEEE Trans. Med. Imaging 18 (8), 712–721.
Salat, D.H., Kaye, J.A., Janowsky, J.S., 1999a. Prefrontal gray and white matter volumes in healthy aging and Alzheimer disease. Arch. Neurol. 56 (3), 338–344.
Salat, D.H., Kaye, J.A., Janowsky, J.S., 2001. Selective preservation and degeneration within the prefrontal cortex in aging and Alzheimer disease. Arch. Neurol. 58 (9), 1403–1408.
Salat, D.H., Stangl, P.A., Kaye, J.A., Janowsky, J.S., 1999b. Sex differences in prefrontal volume with aging and Alzheimer's disease. Neurobiol. Aging 20 (6), 591–596.
Salat, D.H., Tuch, D.S., Greve, D.N., van der Kouwe, A.J., Hevelone, N.D., Zaleta, A.K., Rosen, B.R., Fischl, B., Corkin, S., Rosas, H.D., Dale, A.M., 2005a. Age-related alterations in white matter microstructure measured by diffusion tensor imaging. Neurobiol. Aging 26 (8), 1215–1227.
Salat, D.H., Tuch, D.S., Hevelone, N.D., Fischl, B., Corkin, S., Rosas, H.D., Dale, A.M., 2005b. Age-related changes in prefrontal white matter measured by diffusion tensor imaging. Ann. N. Y. Acad. Sci. 1064, 37–49.
Schmahmann, J., Pandya, D., 2006. Fiber Pathways of the Brain. Oxford University Press, Oxford.
Schmidt, R., Schmidt, H., Kapeller, P., Enzinger, C., Ropele, S., Saurugg, R., Fazekas, F., 2002. The natural course of MRI white matter hyperintensities. J. Neurol. Sci. 203–204, 253–257.
Sjobeck, M., Haglund, M., Englund, E., 2006. White matter mapping in Alzheimer's disease: a neuropathological study. Neurobiol. Aging 27 (5), 673–680.
Smith, S.M., Jenkinson, M., Johansen-Berg, H., Rueckert, D., Nichols, T.E., Mackay, C.E., Watkins, K.E., Ciccarelli, O., Cader, M.Z., Matthews, P.M., Behrens, T.E., 2006. Tract-based spatial statistics: voxelwise analysis of multi-subject diffusion data. Neuroimage 31 (4), 1487–1505.
Smith, S.M., Jenkinson, M., Woolrich, M.W., Beckmann, C.F., Behrens, T.E., Johansen-Berg, H., Bannister, P.R., De Luca, M., Drobnjak, I., Flitney, D.E., Niazy, R.K., Saunders, J., Vickers, J., Zhang, Y., De Stefano, N., Brady, J.M., Matthews, P.M., 2004. Advances in functional and structural MR image analysis and implementation as FSL. Neuroimage 23 (Suppl. 1), S208–S219.
Song, S.K., Sun, S.W., Ju, W.K., Lin, S.J., Cross, A.H., Neufeld, A.H., 2003. Diffusion tensor imaging detects and differentiates axon and myelin degeneration in mouse optic nerve after retinal ischemia. Neuroimage 20 (3), 1714–1722.
Song, S.K., Sun, S.W., Ramsbottom, M.J., Chang, C., Russell, J., Cross, A.H., 2002. Dysmyelination revealed through MRI as increased radial (but unchanged axial) diffusion of water. Neuroimage 17 (3), 1429–1436.
Stern, Y., Hesdorffer, D., Sano, M., Mayeux, R., 1990. Measurement and prediction of functional capacity in Alzheimer's disease. Neurology 40 (1), 8–14.
Stoub, T.R., deToledo-Morrell, L., Stebbins, G.T., Leurgans, S., Bennett, D.A., Shah, R.C., 2006. Hippocampal disconnection contributes to memory dysfunction in individuals at risk for Alzheimer's disease. Proc. Natl. Acad. Sci. U S A 103 (26), 10041–10045.
Stout, J.C., Jernigan, T.L., Archibald, S.L., Salmon, D.P., 1996. Association of dementia severity with cortical gray matter and abnormal white matter volumes in dementia of the Alzheimer type. Arch. Neurol. 53 (8), 742–749.
Sullivan, E.V., Adalsteinsson, E., Hedehus, M., Ju, C., Moseley, M., Lim, K.O., Pfefferbaum, A., 2001. Equivalent disruption of regional white matter microstructure in ageing healthy men and women. Neuroreport 12 (1), 99–104.

Sullivan, E.V., Adalsteinsson, E., Pfefferbaum, A., 2006. Selective age-related degradation of anterior callosal fiber bundles quantified in vivo with fiber tracking. Cereb. Cortex 16 (7), 1030–1039.

Sullivan, E.V., Pfefferbaum, A., 2006. Diffusion tensor imaging and aging. Neurosci. Biobehav. Rev. 30 (6), 749–761.

Swendsen, R.H., Wang, J.S., 1986. Replica Monte Carlo simulation of spin glasses. Phys. Rev. Lett. 57 (21), 2607–2609.

Taoka, T., Iwasaki, S., Sakamoto, M., Nakagawa, H., Fukusumi, A., Myochin, K., Hirohashi, S., Hoshida, T., Kichikawa, K., 2006. Diffusion anisotropy and diffusivity of white matter tracts within the temporal stem in Alzheimer disease: evaluation of the "tract of interest" by diffusion tensor tractography. AJNR Am. J. Neuroradiol. 27 (5), 1040–1045.

Tuch, D.S., 2004. Q-ball imaging. Magn. Reson. Med. 52 (6), 1358–1372.

Tuch, D.S., Reese, T.G., Wiegell, M.R., Makris, N., Belliveau, J.W., Wedeen, V.J., 2002. High angular resolution diffusion imaging reveals intravoxel white matter fiber heterogeneity. Magn. Reson. Med. 48 (4), 577–582.

Van Hoesen, G.W., Hyman, B.T., Damasio, A.R., 1991. Entorhinal cortex pathology in Alzheimer's disease. Hippocampus 1 (1), 1–8.

Vincent, J.L., Snyder, A.Z., Fox, M.D., Shannon, B.J., Andrews, J.R., Raichle, M.E., Buckner, R.L., 2006. Coherent spontaneous activity identifies a hippocampal-parietal memory network. J. Neurophysiol. 96 (6), 3517–3531.

Walhovd, K.B., Fjell, A.M., Reinvang, I., Lundervold, A., Dale, A.M., Eilertsen, D.E., Quinn, B.T., Salat, D., Makris, N., Fischl, B., 2005. Effects of age on volumes of cortex, white matter and subcortical structures. Neurobiol. Aging 26 (9), 1261–1270, discussion 75–8.

Wang, L., Zang, Y., He, Y., Liang, M., Zhang, X., Tian, L., Wu, T., Jiang, T., Li, K., 2006. Changes in hippocampal connectivity in the early stages of Alzheimer's disease: evidence from resting state fMRI. Neuroimage 31 (2), 496–504.